Active control of structural vibration with on-line secondary path modeling*

YANG Tiejun[1, 2**] and GU Zhongquan[2]

(1. Research Institute of Power Plant Technology, Harbin Engineering University, Harbin 150001, China; 2. National Key Laboratory of Rotorcraft and Aeromechanics, Nanjing University of Aeronautics and Astronautics, Nanjing 210016, China)

Received September 2, 2003; revised February 10, 2004

Abstract An active control strategy with on-line secondary path modeling is proposed and applied in active control of helicopter structural vibration. Computer simulations of the secondary path modeling performance demonstrate the superiorities of the active control strategy. A 2-input 4-output active control simulation for a helicopter model is performed and great reduction of structural vibration is achieved. 2-input 2-output and 2-input 4-output experimental studies of structural vibration control for a free-free beam are also carried out in laboratory to simulate a flying helicopter. The experimental results also show better reduction of the structural vibration, which verifies that the proposed method is effective and practical in structural vibration reduction.

Keywords: structural vibration, on-line secondary path modeling, active control.

One of the most popular active control methods is the adaptive active control strategy based on the filtered-x least mean square (x-LMS) algorithm. The basic x-LMS based Active Noise and Vibration Control (ANVC) system is shown in Fig. 1[1], where $\boldsymbol{s}(n)$ is called the secondary path (or error path), which typically comprises the D/A converter, power amplifier, actuator, controlled system, error sensor, preamplifier, A/D converter and so on. One important design of such strategy is the modeling of secondary path.

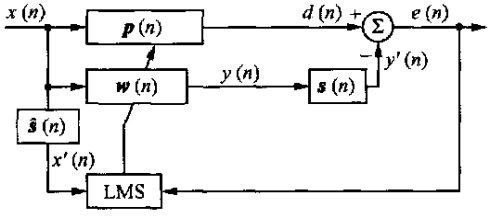

Fig. 1. Basic x-LMS based adaptive control system.

The secondary path, $\boldsymbol{s}(n)$, may be estimated off-line and on-line. Off-line modeling can simplify the control algorithm to a great extent while the system parameters varying slowly or nearly not varying. However, the system characteristics will change with the variation of the operation conditions. Off-line modeling of secondary path cannot satisfy the robust requirement for the control system. It is necessary and practical to model secondary path on-line. There are two different approaches of on-line secondary path modeling, one involves the injection of additional random noise into the ANVC system to utilize a system identification method to model $\boldsymbol{s}(n)$ and the other attempts to model $\boldsymbol{s}(n)$ from the ANVC controller output $y(n)$. A detailed comparison of these two on-line modeling approaches can be found in Ref. 2. The first approach provides a good result since the additional random noise is independent of the primary signal, and the model obtained is valid for the entire frequency range of interest. Although the injection of a random noise will increase the residual noise level, which cannot be suppressed by the controller but can be done by reducing the power of the injection noise. It is pointed out that the first approach is superior to the second one on convergence rate, speed of response to changes of primary noise, computational complexities, etc.[2]. Therefore, only the first approach will be discussed in detail in this paper.

In this paper, an active control strategy with on-line secondary path modeling is proposed and applied in active control of helicopter structural vibration. Comparison with existing methods based on computer simulation of secondary path modeling performance is made, and a 2-input and 4-output active control simulation based on a helicopter model is conducted. Then 2-input 2-output and 2-input 4-output experi-

* Supported by the Aviation Fund (Grant No. 01A52004)

** To whom correspondence should be addressed. E-mail: ytiejun1984@yahoo.com.cn

mental studies of structural vibration control for a free-free beam, which simulates a flying helicopter, are performed in laboratory.

1 Control strategies with on-line secondary path modeling

1.1 Existing methods

An important adaptive algorithm with on-line secondary path modeling was proposed by Eriksson and Allie[3]. In this method (see Fig. 2), a random noise $v(n)$, which is uncorrelated with the primary noise $x(n)$, is injected at the output of the ANVC controller. $v(n)$ is used as the input of the adaptive filter $\hat{\boldsymbol{s}}(n)$ at the same time. When the adaptive process is convergent, the adaptive filter $\hat{\boldsymbol{s}}(n)$ converges to $\boldsymbol{s}(n)$ uniquely. $\boldsymbol{p}(n)$ is the primary path, and $d(n)$ is the system response without control, which is the signal to be reduced and can be called the desired signal, $e(n)$ is the system response with control and is called error signal.

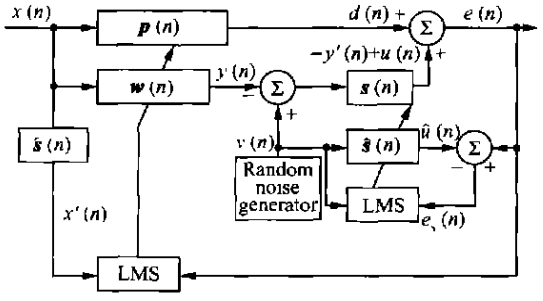

Fig. 2. Eriksson's strategy.

The updating equation of $\hat{\boldsymbol{s}}(n)$ is

$$\begin{aligned}\hat{\boldsymbol{s}}(n+1) &= \hat{\boldsymbol{s}}(n) + \mu_s \boldsymbol{v}(n) e_s(n) \\ &= \hat{\boldsymbol{s}}(n) + \mu_s \boldsymbol{v}(n)(e(n) - \hat{u}(n)) \\ &= \hat{\boldsymbol{s}}(n) + \mu_s \boldsymbol{v}(n)(s(n) * v(n) \\ &\quad - \hat{s}(n) * v(n)) + \mu_s \boldsymbol{v}(n)\eta(n), \end{aligned} \tag{1}$$

where $\eta(n) = d(n) - s(n) * y(n)$, $\hat{\boldsymbol{s}}(n)$ is the estimate of the secondary path $\boldsymbol{s}(n)$ ($\hat{\boldsymbol{s}}(n) = [\hat{s}_0(n), \cdots, \hat{s}_{N-1}(n)]^{\mathrm{T}}$, where N is the length of adaptive filter $\hat{\boldsymbol{s}}(n)$), $\boldsymbol{v}(n)$ is the vector of random noise $v(n)$ ($\boldsymbol{v}(n) = [v(n), \cdots, v(n-N+1)]^{\mathrm{T}}$), and $*$ denotes linear convolution. It can be seen that the adaptive filter $\hat{\boldsymbol{s}}(n)$ converges to the optimal solution $\boldsymbol{s}(n)$ if $v(n)$ is uncorrelated with $x(n)$, but $\mu_s \boldsymbol{v}(n)\eta(n)$ is a perturbation term that can degrade the convergence performance of secondary path modeling. In the worst case, it can cause divergence. $\mu_s \boldsymbol{v}(n)\eta(n)$ reflects the impact of the active control process on the modeling process.

The updating equation of $w(n)$ is

$$\begin{aligned}\boldsymbol{w}(n+1) &= \boldsymbol{w}(n) + \mu_w \boldsymbol{x}'(n) e(n) \\ &= \boldsymbol{w}(n) + \mu_w \boldsymbol{x}'(n)(d(n) \\ &\quad - s(n) * y(n) + u(n)), \end{aligned} \tag{2}$$

where $\boldsymbol{x}'(n) = [x'(n), \cdots, x'(n-L+1)]^{\mathrm{T}}$, $x'(n) = \hat{s}(n) * x(n)$, L is the length of adaptive controller filter $\boldsymbol{w}(n)$, and $u(n) = s(n) * v(n)$. It can be seen that $\mu_w \boldsymbol{x}'(n) u(n)$ will interfere with the updating operation of $\boldsymbol{w}(n)$. The perturbation is proportional to the power of $v(n)$ and is related to $\boldsymbol{s}(n)$. $\mu_w \boldsymbol{x}'(n) u(n)$ reflects the impact of the modeling process on the active control process.

To reduce the undesirable interference introduced by the ANVC controller, $\eta(n)$, when estimating $\boldsymbol{s}(n)$, two improved techniques with on-line secondary path modeling that use the injection of a random noise are proposed by Bao et al.[4] (see Fig. 3) and Kuo et al.[5] The same concept of the two methods is to minimize $\eta(n)$ by using an additional adaptive filter $\boldsymbol{h}(n)$, which is excited by a signal correlated with $x(n)$. The convergence rate of the

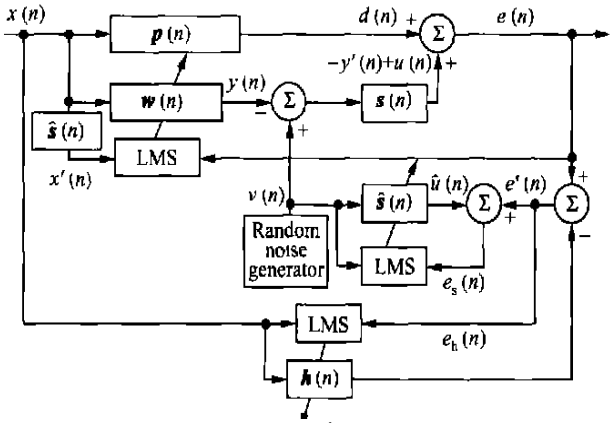

Fig. 3. Bao's strategy.

modeling has been shown to be greatly improved. However, the impact of the modeling process on the active control process, which is caused by $v(n)$, is not considered.

Zhang's method (see Fig. 4) is an improvement of Bao's method[6]. In Zhang's method, three cross-updated least mean square adaptive filters are used to reduce the perturbations between the operation of the ANVC controller and the modeling of secondary path. Computer simulation results demonstrated that superior performance was achieved compared to Bao's method.

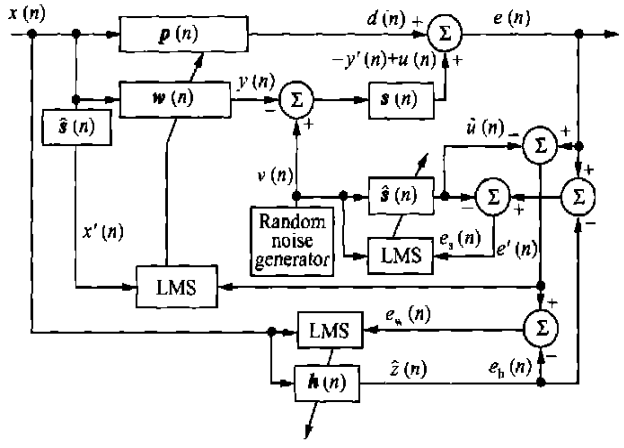

Fig. 4. Zhang's strategy.

1.2 On-line secondary path modeling

A new ANVC system with on-line secondary path modeling based on a set of cross-updated adaptive filters, $\boldsymbol{w}(n)$, $\boldsymbol{h}(n)$ and $\hat{\boldsymbol{s}}(n)$, is proposed here (see Fig. 5). In this method, the output signal $\hat{u}(n)$ ($\hat{u}(n)=\hat{s}(n) * v(n)$) of the filter $\hat{\boldsymbol{s}}(n)$ is subtracted from the signal $e(n)$ to produce a new signal $e_w(n)$ ($e_w(n)=e(n)-\hat{u}(n)$), which is used as the error signal for the controller filter $\boldsymbol{w}(n)$. In the ideal case of when $\hat{\boldsymbol{s}}(n)=\boldsymbol{s}(n)$, $e_w(n)=e(n)-\hat{u}(n)=d(n)-s(n) * y(n)$, the perturbation due to $v(n)$ is totally removed. The updating equation of $\boldsymbol{w}(n)$ now is

$$\boldsymbol{w}(n+1)=\boldsymbol{w}(n)+\mu_w \boldsymbol{x}'(n)e_w(n). \quad (3)$$

As a result, the perturbation caused by $v(n)$ can be greatly reduced. The error signal for the filter $\hat{\boldsymbol{s}}(n)$ and $\boldsymbol{h}(n)$ is

$$e_{sh}(n)=e(n)-\hat{u}(n)-\hat{d}(n)+\hat{y}'(n), \quad (4)$$

where

$$\hat{y}'(n)=\hat{s}(n) * y(n), \quad \hat{d}(n)=h(n) * x(n).$$

The updating equation of $\hat{\boldsymbol{s}}(n)$ now is

$$\begin{aligned}\hat{\boldsymbol{s}}(n+1)&=\hat{\boldsymbol{s}}(n)+\mu_s v(n)e_{sh}(n)\\&=\hat{\boldsymbol{s}}(n)+\mu_s v(n)(e(n)-\hat{u}(n)\\&\quad-\hat{d}(n)+\hat{y}'(n))\\&=\hat{\boldsymbol{s}}(n)+\mu_s v(n)(s(n) * v(n)\\&\quad-\hat{s}(n) * v(n))+\mu_s v(n)\eta'(n),\end{aligned} \quad (5)$$

where

$$\eta'(n)=(d(n)-\hat{d}(n))-(s(n) * y(n)-\hat{s}(n) * y(n)).$$

The updating equation of $\boldsymbol{h}(n)$ now is

$$\begin{aligned}\boldsymbol{h}(n+1)&=\boldsymbol{h}(n)+\mu_h \boldsymbol{x}(n)e_{sh}(n)\\&=\boldsymbol{h}(n)+\mu_h \boldsymbol{x}(n)(e(n)-\hat{u}(n)\\&\quad-\hat{d}(n)+\hat{y}'(n))\\&=\boldsymbol{h}(n)+\mu_h \boldsymbol{x}(n)(d(n)-\hat{d}(n))\\&\quad+\mu_h \boldsymbol{x}(n)\eta''(n)\\&=\boldsymbol{h}(n)+\mu_h \boldsymbol{x}(n)(p(n) * x(n)\\&\quad-h(n) * x(n))+\mu_h \boldsymbol{x}(n)\eta''(n),\end{aligned} \quad (6)$$

where

$$\eta''(n)=(s(n) * v(n)-\hat{s}(n) * v(n))-(s(n) * y(n)-\hat{s}(n) * y(n)).$$

In the ideal case of when $\hat{\boldsymbol{s}}(n)=\boldsymbol{s}(n)$, $\eta''(n)=0$, $\boldsymbol{h}(n)$ will converge to $\boldsymbol{p}(n)$, then $\eta'(n)=0$. It can be seen that the undesirable interference introduced by the ANVC controller, $\eta'(n)$, in the estimation of $\boldsymbol{s}(n)$ will be reduced, so the perturbations between active control process and modeling process can be greatly reduced.

The difference between our proposed method and Zhang's method is the introduction of $\hat{y}'(n)$, the output of $\hat{\boldsymbol{s}}(n)$ due to $y(n)$, into the error signal for the filter $\hat{\boldsymbol{s}}(n)$ and $\boldsymbol{h}(n)$. When it is introduced, any variation due to $y(n)$ is removed from updating

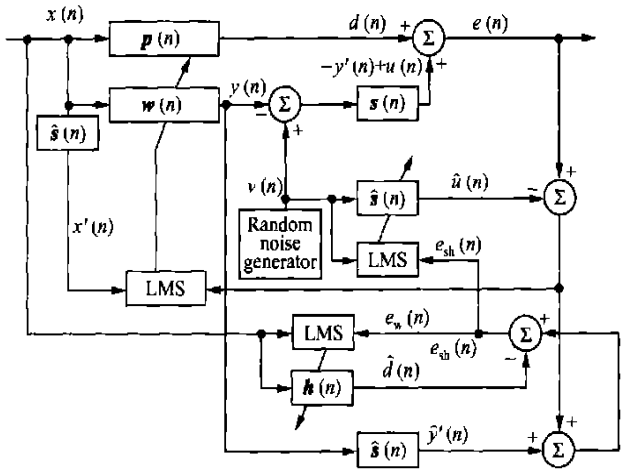

Fig. 5. ANVC system with secondary-path modeling (proposed method).

operations of $\hat{\boldsymbol{s}}(n)$ and $\boldsymbol{h}(n)$. Since $\hat{y}'(n)$ is uncorrelated with $v(n)$, inclusion of the filter copy $\hat{\boldsymbol{s}}(n)$ cannot affect the Wiener solution of the estimated secondary path filter, but the least mean square error of the on-line adaptive modeling process is reduced. Hence, the superior performances can be achieved.

It has been proved in Ref. [7] that the optimal solutions of each estimated filter are as follows:

$$\begin{aligned} S^{*}(z) &= S(z), \\ H^{*}(z) &= P(z) - W^{*}(z)S(z) + W^{*}(z)S(z), \\ W^{*}(z) &= P(z)/S(z), \end{aligned} \tag{7}$$

where $S^{*}(z)$ is the z-transform of $\hat{s}^{*}(n)$, the estimated optimal impulse response of secondary path; $S(z)$ is the z-transform of $s(n)$, the impulse response of secondary path; $H^{*}(z)$ is the z-transform of $h^{*}(z)$, the optimal solution of $h(n)$; $P(z)$ is the z-transform of $p(n)$, and $W^{*}(z)$ is the z-transform of $w^{*}(n)$, the optimal solution of $w(n)$ ($w(n)$ is the impulse response of control filter).

In sum, the total algorithm can be described as

$$\begin{cases} y(n) = w(n) * x(n), \\ \hat{u}(n) = \hat{s}(n) * v(n), \\ \hat{y}'(n) = \hat{s}(n) * y(n), \\ x'(n) = \hat{s}(n) * x(n), \\ \hat{d}(n) = h(n) * x(n), \\ e_{w}(n) = e(n) - \hat{u}(n), \\ e_{sh}(n) = e(n) - \hat{u}(n) - \hat{d}(n) + \hat{y}'(n), \\ \boldsymbol{w}(n+1) = \boldsymbol{w}(n) + \mu_{w}\boldsymbol{x}'(n)e_{w}(n), \\ \hat{\boldsymbol{s}}(n+1) = \hat{\boldsymbol{s}}(n) + \mu_{s}v(n)e_{sh}(n), \\ \boldsymbol{h}(n+1) = \boldsymbol{h}(n) + \mu_{h}\boldsymbol{x}(n)e_{sh}(n). \end{cases} \tag{8}$$

Simulations of on-line secondary path modeling performance has been conducted based on a two-stage active vibration isolation system[7]. An 8-order FIR filter is used to model secondary path of the active vibration isolation system here. Fig. 6 shows the modeling process by off-line modeling method. The differences of each weight of estimated secondary path between our proposed on-line method and off-line method with the same convergence coefficient is shown in Fig. 7. The processes start at the 5th second. As the process goes on, the differences tend to be zero. It can be seen that the modeling precision of our proposed method is close to that of off-line method.

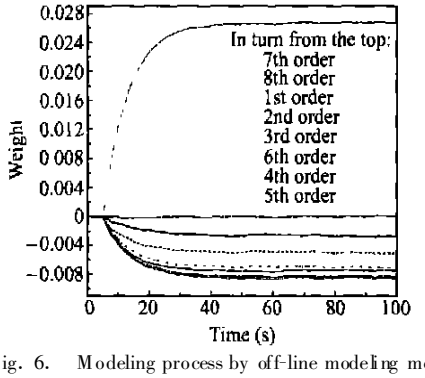

Fig. 6. Modeling process by off-line modeling method.

To compare the proposed method and Zhang's method, the secondary path estimated performance is defined as the sum of squared error of 8 weights between on-line method and off-line method. Fig. 8 shows comparison of the estimated performance between the proposed method and Zhang's method with the same convergence coefficients. It can be seen that the proposed method gives better results than Zhang's method.

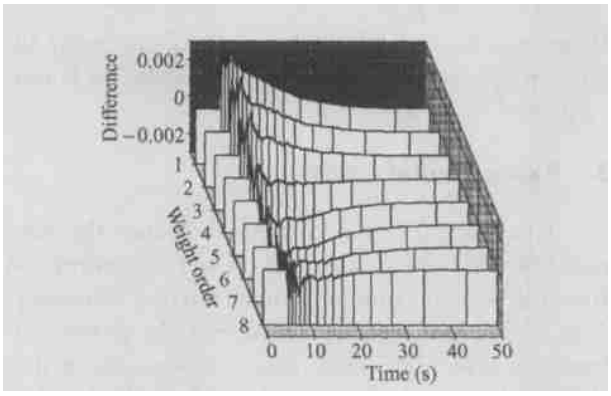

Fig. 7. Differences of each weight of estimated secondary path between the proposed method and off-line method.

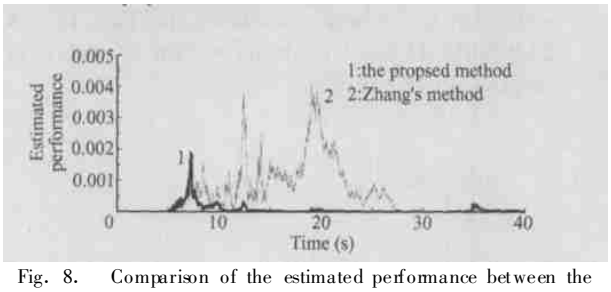

Fig. 8. Comparison of the estimated performance between the proposed method and Zhang's method.

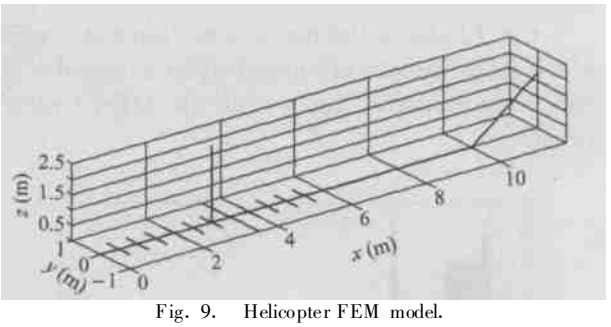

Fig. 9. Helicopter FEM model.

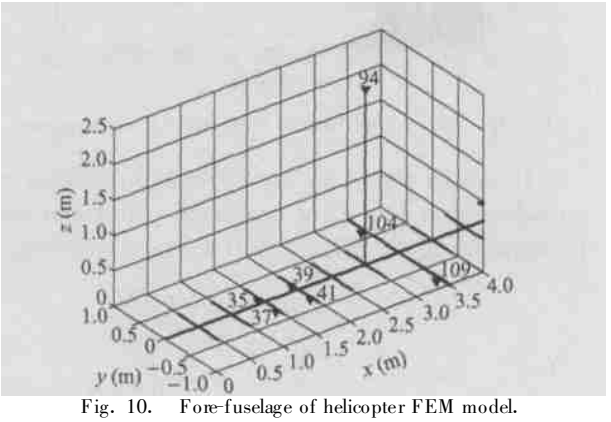

Fig. 10. Fore-fuselage of helicopter FEM model.

2 Numerical simulation

2.1 A helicopter model

The helicopter model is constructed based on the finite element method with ANSYS, as shown in Fig. 9. Fig. 10 shows the nodes arrangement at the fore-fuselage. External excitation disturbance is introduced from the 94th node, control force is introduced from nodes 104, 109, and vibration signals are picked up from nodes 35, 37, 39, and 41 as error signals.

2.2 2-input 4-output control simulation

Some computer simulations have been conducted to evaluate the performance of the proposed method. The disturbance, which is defined as

$$f = 1500\sin(2\pi \times 17 \times t) + 750\sin(2\pi \times 34 \times t)\text{N},$$

is input at node 94. The controller, secondary path and parallel path are modeled by 64-order FIR filters with zero initial values. The power ratio of the primary noise and the injected noise at the error sensors can be computed to be about 25. The step sizes for updating controller filters, secondary path modeling filters and parallel path modeling filters are all 0.0001, the sampling frequency is set to be 1000Hz. The control process starts at the 10th second. Fig. 11 shows the vibration control process of the four error evaluation nodes.

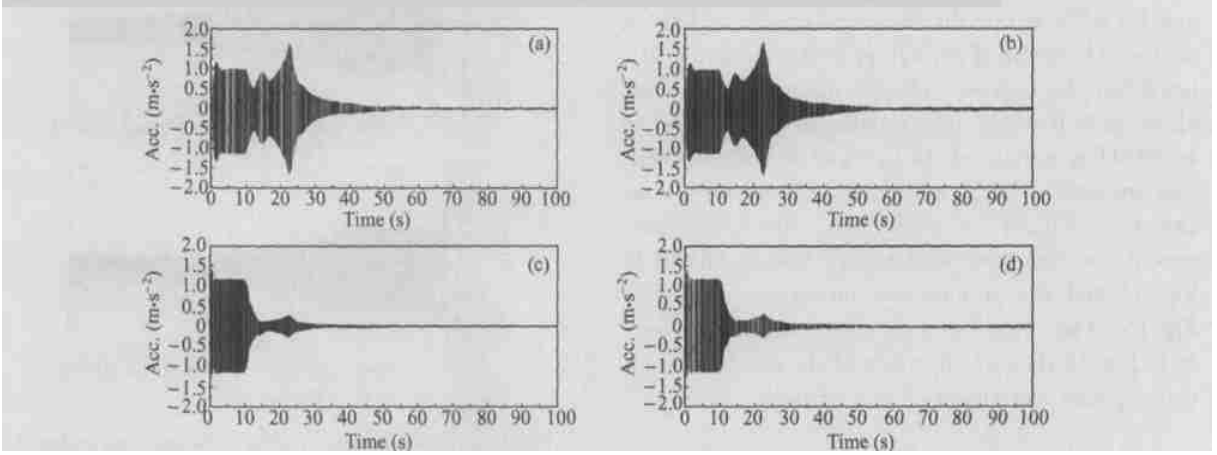

Fig. 11. Control process of the four error evaluation points. (a) Acceleration response of node 35; (b) acceleration response of node 37; (c) acceleration response of node 39; (d) acceleration response of node 41.

Fig. 12 shows the performance function, which is defined as the sum of squared vibration signal of the four error evaluation points, of the MIMO control system.

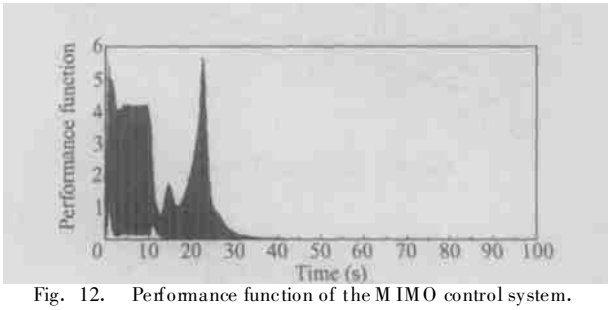

Fig. 12. Performance function of the MIMO control system.

It can be seen that good vibration attenuations are achieved at four error evaluation points and good performance of the MIMO control system is confirmed. It can also be observed that outputs of controller filters are nearly stable when the control system is convergent.

3 Experimental study

Experimental investigations utilizing the proposed method are carried out in our laboratory. A free-free beam is hung to simulate a flying helicopter. It is excited by a primary actuator as the primary vibration source. Two proof-mass actuators are used as secondary sources to control two or four error evaluation points. The schematic diagram of the 2-input 4-output control system is shown in Fig. 13. A TMS320VC33-based hardware system is applied as adaptive active controller.

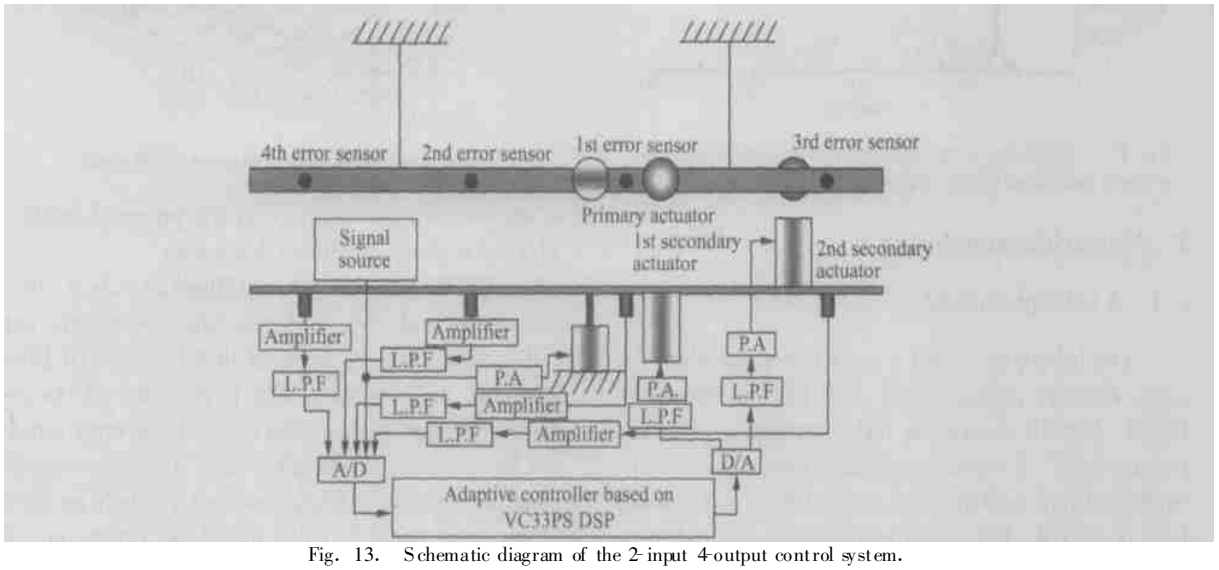

Fig. 13. Schematic diagram of the 2-input 4-output control system.

3.1 2-input 2-output control experiment

A dual-frequency disturbance containing 12.1 Hz and 14.6 Hz is introduced as the primary vibration source. The order of each filter with zero initial values is 64, the step sizes of each updating process are all set to be 0.0001, the sampling frequency is set to be 1000 Hz, outputs of the first and second error sensors are used as error evaluation, the adaptive controller is a 2-input 2-output system. The control process of the two error evaluation points is shown in Fig. 14 and the performance function is shown in Fig. 15. The control process starts at the 65th second. Fig. 16 shows comparison of the two error evaluation points vibration with and without control.

It can be confirmed that both contents of primary vibration are greatly attenuated.

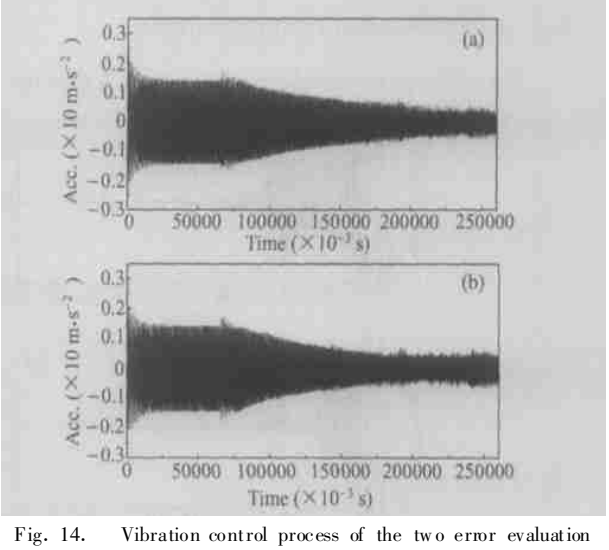

Fig. 14. Vibration control process of the two error evaluation points of free-free beam. (a) Output of the first error sensor; (b) output of the second error sensor.

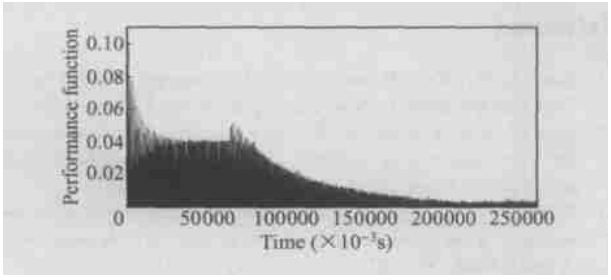

Fig. 15. Performance function of the 2I2O adaptive control system.

3.2 2-input 4-output control experiment

The schematic diagram of the 2-input 4-output control system is shown in Fig. 15. A 12 Hz disturbance is introduced. The order of each filter is also 64, the step sizes of each updating process are all set to be 0.00003, the sampling frequency is still set to be 1000 Hz. The control processes of the four error evaluation points are shown in Fig. 17, and the performance function is shown in Fig. 18. The diagrams are drawn when the control system begins to converge.

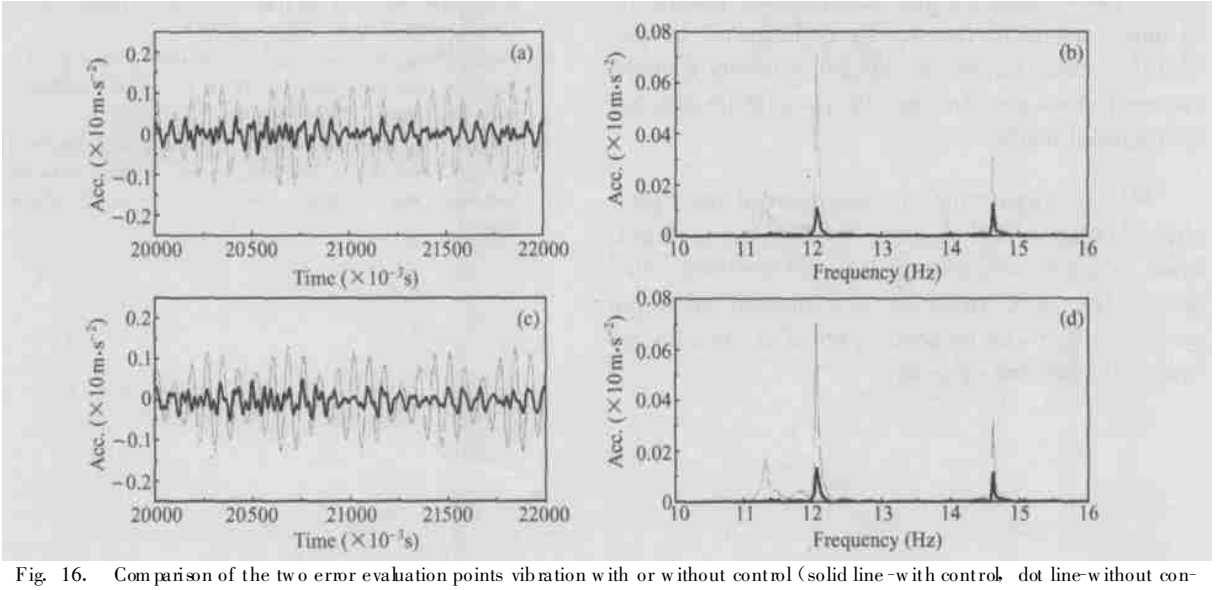

Fig. 16. Comparison of the two error evaluation points vibration with or without control (solid line-with control, dot line-without control). (a) and (b), Output of the first error sensor; (c) and (b), output of the second error sensor.

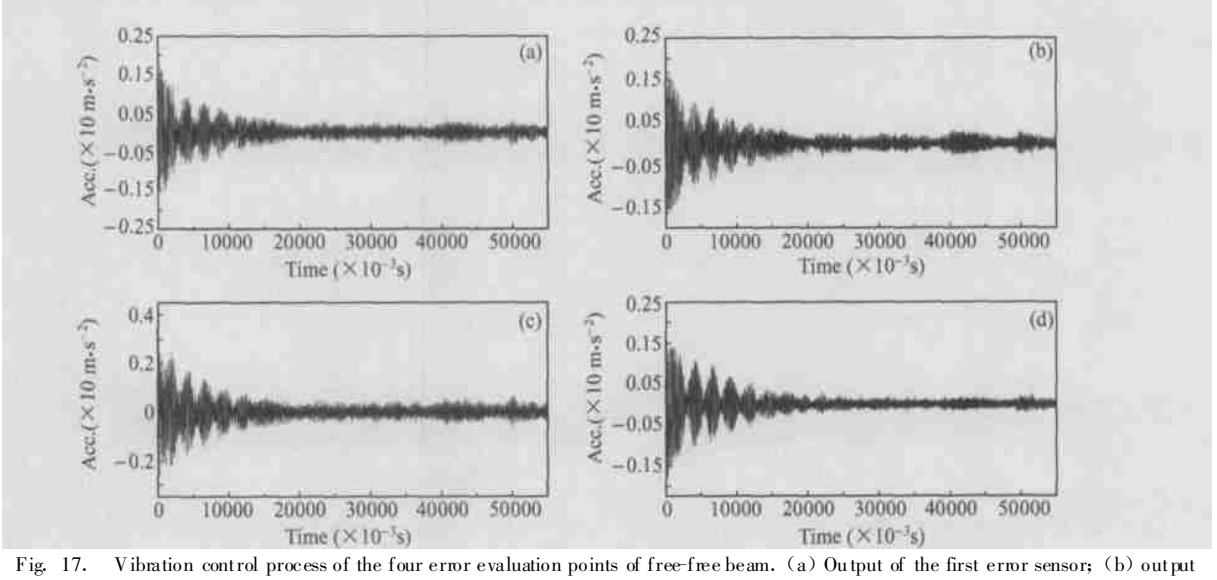

Fig. 17. Vibration control process of the four error evaluation points of free-free beam. (a) Output of the first error sensor; (b) output of the second error sensor; (c) output of the third error sensor; (d) output of the fourth error sensor.

4 Conclusions

In this paper, a new ANVC system with on-line secondary path modeling has been presented. With the construction of filters, the proposed system can greatly reduce the mutual disturbances between the

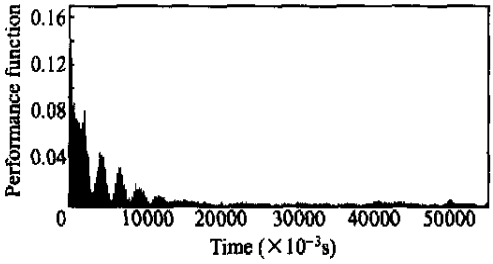

Fig. 18. Performance function of the 2-input 4-output adaptive control system.

control process and the modeling process, leading to an improvement in the overall performance of the ANVC system. Computer simulation results support the conclusions and demonstrate the effectiveness of the proposed method.

MIMO experimental investigations of the structural vibration control of a free-free beam simulating a flying helicopter are performed in our laboratory. The results show good reduction of structural vibration and verify that our proposed method is effective in structural vibration reduction.

References

1 Kuo, S. M. et al. Active Noise Control Systems: Algorithms and DSP Implementations. New York: John Wiley & Sons, 1996.
2 Bao, C. et al. Comparison of two on-line identification algorithms for active noise control. In: Proc. Recent Advances in Actice Control of Sound Vibration, 1993, 38.
3 Eriksson, L. J. et al. Use of random noise for online transducer estimate in an adaptive attenuation system. J. Acoust. Soc. Amer., 1989, 85: 797.
4 Bao, C, et al. Adaptive active control of noise in 3-D reverberant enclosures. J. Sound Vibr., 1993, 161: 501.
5 Kuo, S. M. et al. Multiple-channel error path modeling with the interchannel decoupling algorithm. In: Proc. Recent Advances in Actice Control of Sound Vibration, 1993.
6 Zhang, M. et al. Cross-updated active noise control system with online secondary path modeling. IEEE Transactions on Speech and Audio Processing, 2001, 9(5): 598.
7 Yang, T. J. Study on adaptive vibration control for helicopter structure. Post Doctor Research Report, Nanjing University of Aeronautics and Astronautics, Nanjing, P. R. C. (in Chinese), 2003.